

Portland State University

**PDXScholar**

---

Civil and Environmental Engineering Faculty  
Publications and Presentations

Civil and Environmental Engineering

---

2-1-2009

# Evolution of Tidal Amplitudes in the Eastern Pacific Ocean

David A. Jay

*Portland State University*, [djay@pdx.edu](mailto:djay@pdx.edu)

Follow this and additional works at: [https://pdxscholar.library.pdx.edu/cengin\\_fac](https://pdxscholar.library.pdx.edu/cengin_fac)



Part of the [Civil and Environmental Engineering Commons](#)

**Let us know how access to this document benefits you.**

---

## Citation Details

Jay, D. A. (2009), Evolution of tidal amplitudes in the eastern Pacific Ocean, *Geophys. Res. Lett.*, 36, L04603

This Article is brought to you for free and open access. It has been accepted for inclusion in Civil and Environmental Engineering Faculty Publications and Presentations by an authorized administrator of PDXScholar. Please contact us if we can make this document more accessible: [pdxscholar@pdx.edu](mailto:pdxscholar@pdx.edu).

## Evolution of tidal amplitudes in the eastern Pacific Ocean

David A. Jay<sup>1</sup>

Received 30 September 2008; revised 10 December 2008; accepted 16 January 2009; published 19 February 2009.

[1] Global sea level (GSL) rise is well documented. However, changes in high waters, including the tidal contribution, are sometimes more relevant than GSL rise. Analysis of 34 long tidal records from the Eastern Pacific Ocean shows that  $K_1$  and  $M_2$  amplitudes ( $|K_1|$  and  $|M_2|$ ) are increasing, except for  $|M_2|$  in the Gulf of Panama. North of 18°N,  $|K_1|$  and  $|M_2|$  are both growing at 2.2% century<sup>-1</sup>. The mean increase in total tidal amplitude (0.59 mmyr<sup>-1</sup>) is less than the present GSL rise (1.7 mmyr<sup>-1</sup>). However, mean sea level is nearly constant in the NE Pacific, so tidal evolution plays a major regional role in changes in high water levels. The spatial pattern of tidal evolution suggests the influence of large-scale processes, and the similarity in spatial patterns for  $|K_1|$  and  $|M_2|$  excludes mechanisms with strong frequency dependence. Increasing tidal amplitudes may impact ocean mixing, nutrient supply, primary production, fisheries, and coastal erosion. **Citation:** Jay, D. A. (2009), Evolution of tidal amplitudes in the eastern Pacific Ocean, *Geophys. Res. Lett.*, 36, L04603, doi:10.1029/2008GL036185.

### 1. Introduction and Background

[2] Global sea level (GSL) is rising at  $\sim 1.7$  mmyr<sup>-1</sup> and accelerating at  $\sim 0.01$  mmyr<sup>-2</sup> [Church and White, 2006; Jevrejeva et al., 2008]. With respect to coastal inundation, however, the height of the highest high waters, the sum of local sea level (MSL) and tidal amplitude, is more relevant than MSL alone. In contrast to GSL, tides are usually thought of as stationary, even though their astronomical forcing changes slowly [Cartwright and Eden, 1973], and tidal datum levels are evolving in geographically variable ways that imply changes in both GSL and tidal processes [Flick et al., 2003].

[3] Previous studies have defined long-term changes in tides at individual ports [Cartwright, 1972] and examined tidal evolution in Northern Europe [Woodworth et al., 1991]. Bowen [1972] and Amin [1983] show that human alteration of harbors can be a dominant factor, while Pugh [1982] suggests GSL-rise driven movement of amphidromic points as the cause of changes in the Irish Sea. Ray [2006] documents a slow increase in  $M_2$  in the Gulf of Maine followed by a sharp offset downward; causes are unclear. Colosi and Munk [2006] argue that an increase in  $M_2$  tidal amplitude at Honolulu has been caused by a change in phase of the  $M_2$  internal tide associated with large-scale changes in stratification. Thus, tides are evolving at many locations (sometimes rapidly), and we lack a clear picture of

the dominant causes of the observed changes, a significant gap in our understanding of tides.

[4] A broader understanding of the mechanisms and importance of the evolution of coastal tides requires determination of the spatial structure of this evolution, considering the amphidromal organization of tides. The analysis is best carried out in an area with a narrow continental shelf that minimizes direct effects of GSL rise on tidal amplitudes [Pugh, 1982] that scale with the relative depth change. Most tide gauges are located in harbors, and some impact of harbor alteration is unavoidable. Thus, it is important to examine records from as many gauges as possible. The Eastern Pacific is a good setting for an analysis of tidal evolution, because many harbors are not heavily developed, and the shelf is narrow along most of its length. Also, GSL has been nearly constant since 1970 in the Northeast Pacific [Jevrejeva et al., 2006].

[5] This study documents widespread increases in the amplitudes of the largest diurnal ( $K_1$ ) and semidiurnal ( $M_2$ ) constituents in the Eastern Pacific from Chile to Alaska (33°S to 60°N latitude). The only systematic exception is  $M_2$  from 12°S to 18°N. This amphidromal organization of tidal evolution suggests that large-scale changes in oceanic processes are occurring, though modified by harbor development. This contribution determines the regional rate of tidal evolution and shows that records <40–50 yrs LOR (length of record) do not adequately define trends in tidal properties. Previously described mechanisms are unlikely to explain all of the observed changes; two possible additional causes are suggested.

### 2. Data and Methods

[6] Elevation records from 70 coastal stations between 33°S to 61°N latitude were analyzed. (Data sources, station selection, analysis methods, results, and the influence of record length are described in the auxiliary material).<sup>1</sup> Three amphidromes impinge on the coast in this region for both  $K_1$  and  $M_2$ . As described below, determination of trends in tidal properties is based on the 34 stations with LOR >44 yrs (Figure 1). Unavoidably, some are distant from the open ocean (e.g., Seattle, 47.6°N) or in heavily altered systems (e.g., Astoria, 46.2°N). In cases where abrupt changes in tidal properties were correlated with specific harbor developments, the record before the change was excluded.

[7] Four methods were used to extract changes in the amplitude and phase of the largest diurnal ( $K_1$ ) and semidiurnal ( $M_2$ ) constituents. All gave similar results. Results presented here are based on a complex demodulation (filter length 26,283 hrs, or  $\sim 3$  yrs) of the hourly data and astronomical tidal potential for each station using filters

<sup>1</sup>Department of Civil and Environmental Engineering, Portland State University, Portland, Oregon, USA.

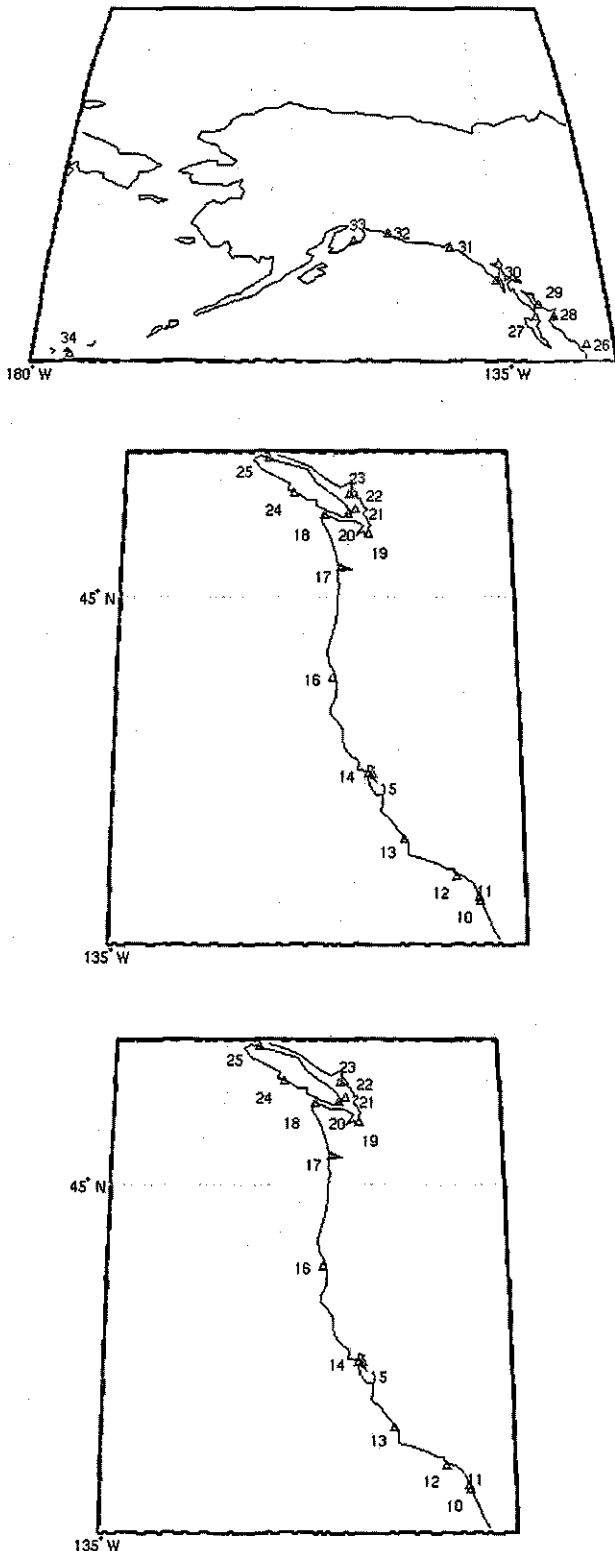


**Figure 1.** Locations of long-term tide stations. See color version of this figure in the HTML.

tuned to  $K_1$  and  $M_2$ . A complex admittance, a ratio of the tidal response to the tidal potential, was then computed for  $K_1$  and  $M_2$ . The changing tidal response over time was determined by regression of the resulting annual admittance amplitude ratios and phase differences against time. Only

constituent amplitudes (denoted  $|K_1|$  and  $|M_2|$ ), with 95% confidence limits, are presented here because amplitudes are more relevant to coastal inundation. A local MSL trend was also estimated, using regression of annual outputs from convolution of the hourly data with a 3yr low-pass filter. The influence of long-term changes in astronomical forcing was taken into account by calculation of the tidal potential with a routine provided by Dr. R. Ray (personal communication, 2009) that incorporates the time-evolution of the tidal potential, which is, however, much smaller than the estimated rates of change.

[8] Determining the minimum useful LOR for defining tidal evolution is crucial. The MSL spectrum exhibits decadal variations that dominate MSL fluctuations in records with  $<50$  yrs LOR [Douglas, 1992]. The constituent amplitude spectrum is different, with considerable energy at  $\sim 9$  and 18.6 yrs, especially for  $K_1$ . The influence of these variations is largely removed through use of the admittance amplitude, because these frequencies appear in both the observations and tidal potential. Analyses of all 28, 37, 47, 56 and 65 yr contiguous sub-sets for six stations with  $LOR > 80$  yrs were used to determine the effect of LOR and unresolved nodal variations on the inferred constituent trends. At several stations, a qualitative shift in analysis behavior occurred at 47–56 yrs. Shorter records sometimes yield trend estimates that depend on the starting year relative to the 18.6 yr nodal cycle. Still, it is possible for 65 yr subsets to show changes in sign, if the constituent trend is weak. Thus, multiple stations are needed to judge the spatial distribution of changes in tidal processes. Balancing the need for long records with the realities of station distribution, results presented here are based on 34 stations with  $LOR > 44$  yrs.

[9] The total growth rate of high water elevations is estimated as the sum of the MSL rise and total tidal change rates. Because catastrophic inundation is often associated with the coincidence of a storm surge with a very high tide, the total tidal rate is the sum of the  $D_1$  and  $D_2$  rates ( $|D_1| + |D_2|$ ), assuming that the two waves are in phase. The  $D_1$  rate is the sum of the rates for  $|K_1|$ ,  $|O_1|$  and  $|P_1|$ . The  $D_2$  rate is the sum of the rates for  $|M_2|$ ,  $|S_2|$ ,  $|N_2|$  and  $|K_2|$ . Only the  $|K_1|$  and  $|M_2|$  rates were actually calculated. Rates for the other constituents were estimated, assuming that both the admittance and growth rate are constant within each species. The total  $|D_1|(|D_2|)$  rate is then 2.04(1.78) times the  $|K_1|(|M_2|)$  rate. This total tidal growth rate is approximate, because there are variations in growth rate between constituents within a species [Ray, 2006].

### 3. Results

[10] The spatial distributions of  $|K_1|$  and  $|M_2|$  are presented first (Figure 2). (Stations are ordered based on the sense of Kelvin wave propagation in the northern hemisphere; station latitudes are also shown.) Inland waters aside,  $|K_1|$  increases from the equator northward, from 0.11 m to 0.4–0.55 m (Figure 2a). Maximum  $|K_1|$  values of 0.64–0.87 m occur in inland waters between 47.7 and 50°N.  $|M_2|$  is large ( $>1.1$  m) near the equator (1.8–9°N) and in the Gulf of Alaska (51–61°N), with a secondary peak at Seattle at 47.6°N (Figure 2b).  $|K_1|$  and  $|M_2|$  both increase modestly south from the equator. The spatially uniform

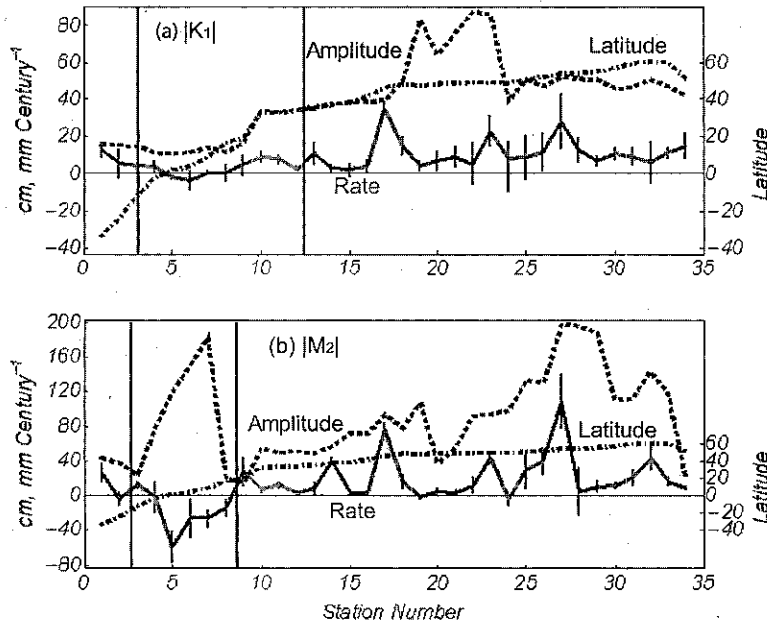


**Figure 2.** Spatial distribution of amplitude (cm) and amplitude trend ( $\text{mmcentury}^{-1}$ ) for (a)  $K_1$  and (b)  $M_2$  by station number; station latitude, 95% confidence limits, and amphidrome boundaries are also shown. See color version of this figure in the HTML.

18.6 yr cycle amplitudes are  $11.2 \pm 0.2\%$  and  $3.6 \pm 0.1\%$  of  $|K_1|$  and  $|M_2|$ , respectively.

[11] Absolute  $|K_1|$  and  $|M_2|$  growth rates (with 95% confidence limits) are shown in Figures 2a and 2b. Also shown are approximate demarcations of the tidal amphidromes [Pugh, 2004]. The  $|K_1|$  trend is small but generally positive in the Equatorial amphidrome between  $12^\circ\text{S}$  and  $35^\circ\text{N}$ , and uniformly positive (though not all results are significant at the 95% level) both south of  $12^\circ\text{S}$  and north of  $35^\circ\text{N}$  (in the South and Northeast Pacific amphidromes). The maximum  $|K_1|$  rate occurs at Astoria ( $46.2^\circ\text{N}$ ). The  $|M_2|$  trend is negative in the Gulf of Panama amphidrome between  $15^\circ\text{S}$  and  $18^\circ\text{N}$ , and almost uniformly positive (though not always significantly so) north of  $18^\circ\text{N}$  (in the Northeast Pacific amphidrome). There are too few stations to determine a trend in South America. Maximum  $|M_2|$  growth rates are seen at San Francisco ( $37.8^\circ\text{N}$ ), Astoria and at Queen Charlotte City ( $54.3^\circ\text{N}$ ); the first two gauges are in strongly altered systems.

[12] The relative growth rates of  $|K_1|$  and  $|M_2|$  (the absolute growth rate normalized at each station by the

amplitude) are shown in Figure 3. There is a striking similarity in the two, with the exception of anomalous  $|M_2|$  values at Acapulco and Manzanillo ( $16.8$  and  $19.1^\circ\text{N}$ ). While both stations have  $\text{LOR} > 44\text{yrs}$ , each has extensive gaps. Considering only stations north of Manzanillo, the mean relative  $|K_1|$  and  $|M_2|$  trends are  $2.2 \pm 0.7$  and  $2.2 \pm 0.9\% \text{century}^{-1}$ , respectively. These values emphasize both the similarity in patterns between species and the size of the changes that are occurring – at present rates, the average time for a doubling of tidal amplitudes is  $\sim 4,500$  yrs. Figure 3 also suggests that one should seek mechanisms that do not strongly discriminate between the  $K_1$  and  $M_2$  frequencies. This appears to exclude phenomena related to internal tides (as traditionally understood), because linear  $K_1$  internal tides do not propagate poleward of  $30^\circ\text{N}$ , but both the  $|K_1|$  and  $|M_2|$  rates are maximal north of  $30^\circ\text{N}$ .

[13] The relative importance of MSL rise and tidal evolution can be compared using Figure 4, which shows  $(|D_1| + |D_2|)$ ,  $(|D_1| + |D_2|) + \text{MSL}$ , and  $\text{GSL}$ . For summary purposes, the results are separated into two segments: the

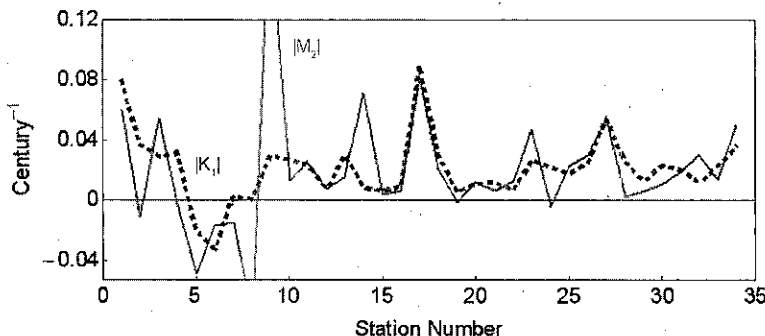


**Figure 3.** Spatial distribution of relative amplitude trend ( $\text{century}^{-1}$ ) for  $K_1$  and  $M_2$  by station number. See color version of this figure in the HTML.

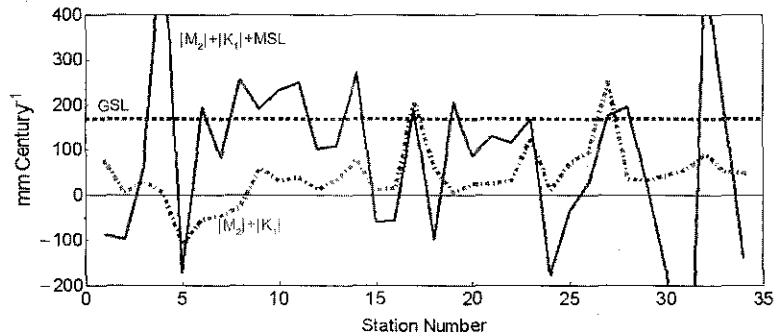


**Figure 4.** Total tidal ( $|D_1| + |D_2|$ ), total tidal plus MSL ( $(|D_1| + |D_2|) + \text{MSL}$ ), and GSL trends ( $\text{mmcentury}^{-1}$ ). See color version of this figure in the HTML.

Gulf of Panama (stations 3–8) and the Northeast Pacific (stations 10–34, dropping Manzanillo). The GSL rise rate ( $1.7 \text{ mmyr}^{-1}$ ) is greater than almost all but two of  $|D_1| + |D_2|$  values for the 25 NE Pacific stations. However, the present (post-1970) average NE Pacific rate of MSL rise is near zero [Jevrejeva *et al.*, 2006]. Thus, the mean total ( $|D_1| + |D_2|$ ) growth rate of tidal amplitudes ( $0.59 \pm 0.23 \text{ mmyr}^{-1}$ ) dominates changes in extreme high water elevations in the NE Pacific. Because of the diverse tectonic settings of the various tide stations in the area, variations between stations are large. At some stations, for example, a negative MSL rate is partially offset by a positive value of  $|D_1| + |D_2|$ . In contrast  $|K_1|$  is generally increasing and  $|M_2|$  decreasing in the Gulf of Panama. Here, the average MSL rate is  $2.1 \pm 0.25 \text{ mm yr}^{-1}$ , while  $(|D_1| + |D_2|)$  is  $-0.33 \pm 0.51 \text{ mm yr}^{-1}$ . Thus, in the Gulf of Panama, tidal evolution is a small part of the entire picture.

[14] The nodal cycle plays a role in variations of coastal and ocean mixing, and may also influence climate fluctuations [Yasuda *et al.*, 2006; Keeling and Whorf, 1997; Ray, 2007]. Therefore, the absolute value of a constituent trend divided by the amplitude of its 18.6 yr cycle also provides a relevant time scale – the length of time over which tidal evolution will compensate for the amplitude of the present 18.6 yr cycle. In this case, the rates for the Gulf of Panama and the Northeast Pacific are similar: 320–360 yrs for  $|M_2|$  and 1,120–1,170 yrs for  $|K_1|$ . The longer time scale for  $|K_1|$  reflects the larger 18.6 yr cycle. Relative to the time scales of deep-ocean mixing (thousands of years), tidal evolution is rapid.

#### 4. Implications and Conclusions

[15] One vital aspect of increasing tidal amplitudes is its contribution to coastal inundation and erosion. Neglecting tsunamis, extreme coastal inundation results from the coincidence of tidal and atmospheric effects, the latter including both storm surge and waves. Wave heights are generally increasing along the US West Coast, and extreme ENSO conditions may bring severe storms [Allan and Komar, 2006], with El Niño conditions temporarily increasing MSL by 0.1–0.3 m. The variability of tidal evolution rates indicates that tidal impacts on coastal erosion will be regionally variable. Increased coastal inundation appears to be especially likely north of  $\sim 40^\circ\text{N}$ , where wave amplitudes are also increasing and MSL rise is quite variable. The

relatively rapid tidal growth rate in parts of the Northeast Pacific amphidrome, especially off Oregon and Alaska, may also alter estuarine, coastal and larger-scale vertical mixing, possibly affecting nutrient supply, primary production and fisheries.

[16] The causes of the observed tidal evolution beg investigation. Small-scale processes (harbor modification, internal tides and coastal trapped waves) may impact some stations but cannot produce the observed amphidromic-scale changes. Whatever the cause, a shift in the location of amphidromic points seems the most probable explanation for the observed spatial pattern. But what would drive such a change? Two mechanisms seem possible, both outside the limits of the traditional Laplace tidal equations (LTE) that do not consider either stratification effects or interactions with wind-driven motions. Actual barotropic tides are coupled to internal tides and stratification effects in a number of ways, e.g., through boundary interactions, turbulent mixing, and the “non-traditional” Coriolis terms. Gerkema *et al.* [2008] show that inclusion of all Coriolis terms greatly increases the latitudinal range in which internal diurnal waves are allowed. Arbic *et al.* [2004] note that global tidal simulations are improved by including internal tides via a two-layer model. The improvement is not due to surface manifestations of the internal tide, but due “to a shift in the barotropic tide induced by baroclinicity.” Thus, changes in stratification near topography, acting through boundary effects and/or non-traditional Coriolis terms, could affect tidal amplitudes.

[17] Kolker and Hameed [2007] suggest that shifting of atmospheric centers of action in part drives GSL rise. Similarly, large-scale changes in wind-driven circulation might alter the mean vorticity of the upper ocean, changing the effective background vorticity gradient in which tidal waves propagate. A scale analysis suggests that such a mechanism is possible. Assume that tidal evolution is the result of a shift in amphidromic point locations. If elevation varies linearly away from an amphidromic point 2000 km from a coast, then a  $2\% \text{century}^{-1}$  change in tidal amplitude implies a  $40 \text{ km century}^{-1}$  shift in amphidromic point location. If we consider the West-Wind Drift at  $50^\circ\text{N}$ , the planetary vorticity gradient is  $\partial f/\partial y \approx 3 \times 10^{-12} (\text{ms})^{-1}$ . A reasonable vorticity due to wind driven circulation is  $\omega = \partial u/\partial y \sim 10^{-7} \text{ s}^{-1}$ . In general,  $\partial \omega/\partial y$  is likely to be  $\ll \partial f/\partial y$ , but  $\omega$  changes sign across the West-Wind Drift. If this occurs over  $\sim 100 \text{ km}$ , then locally,  $\partial \omega/\partial y \approx 10^{-12} (\text{ms})^{-1}$ . Thus, a  $\sim 3\%$  change in  $\partial \omega/\partial y$  would cause a 1% change in

the total vorticity gradient  $\partial(f + \omega)/\partial y$ . Could such a local change in  $\partial\omega/\partial y$  alter by 40 km the position of tidal amphidromic points? Modeling will be required to provide an answer. The two mechanisms of tidal evolution suggested here are both climate-related and speculative. It remains unclear, therefore, whether rapid evolution of tidal amplitudes can be described as a symptom of global climate change.

[18] **Acknowledgments:** This research was funded by National Science Foundation grant OCE-0239072. I thank all those who provided data: L. Hickman, S. Lyles and C. Zervas (National Oceanic and Atmospheric Administration), R. Thomson (Institute of Ocean Sciences), P. Caldwell and B. Kilonsky (University of Hawaii Sea Level Center), A. Gibbs (US Geological Survey), and the Canadian Marine Environmental Data Service. R. Ray of the National Aeronautical and Space Administration provided a routine for calculating tidal potential. Thanks to Ed Zaron for discussions regarding the causes of tidal evolution.

## References

- Allan, J. C., and P. D. Komar (2006), Climate controls on US west coast erosion processes, *J. Coastal Res.*, 22, 511–529.
- Amin, M. (1983), On perturbations of harmonic constants in the Thames estuary, *Geophys. J. R. Astron. Soc.*, 73, 587–603.
- Arbic, B. K., S. T. Garner, R. W. Hallberg, and H. L. Simmons (2004), The accuracy of surface elevations in forward global barotropic and baroclinic tide models, *Deep Sea Res., Part II*, 51, 3069–3101.
- Bowen, A. J. (1972), The tidal regime of the river Thames; long-term trends and their possible causes, *Philos. Trans. R. Soc. London, Ser. A*, 272, 187–199.
- Cartwright, D. (1972), Secular changes in the oceanic tides at Brest, *Geophys. J. R. Astron. Soc.*, 30, 433–449.
- Cartwright, D., and A. C. Eden (1973), Corrected table of tidal harmonics, *Geophys. J. R. Astron. Soc.*, 33, 253–264.
- Church, J. A., and N. J. White (2006), A 20th century acceleration in global sea-level rise, *Geophys. Res. Lett.*, 33, L01602, doi:10.1029/2005GL024826.
- Colosi, J. A., and W. Munk (2006), Tales of the venerable Honolulu tide gauge, *J. Phys. Oceanogr.*, 36, 967–996, doi:10.1175/JPO2876.1.
- Douglas, B. C. (1992), Global sea level acceleration, *J. Geophys. Res.*, 97, 12,699–12,706.
- Flick, R. E., J. F. Murray, and L. C. Ewing (2003), Trends in United States tidal datum statistics and tide range, *J. Waterw. Port Coastal Ocean Eng.*, 124, 155–164.
- Gerkema, T., J. T. F. Zimmerman, L. R. M. Maas, and H. van Haren (2008), Geophysical and astrophysical fluid dynamics beyond the traditional approximation, *Rev. Geophys.*, 46, RG2004, doi:10.1029/2006RG000220.
- Jevrejeva, S., A. Grinsted, J. C. Moore, and S. Holgate (2006), Nonlinear trends and multiyear cycles in sea level records, *J. Geophys. Res.*, 111, C09012, doi:10.1029/2005JC003229.
- Jevrejeva, S., J. C. Moore, A. Grinsted, and P. L. Woodworth (2008), Recent global sea level acceleration started over 200 years ago?, *Geophys. Res. Lett.*, 35, L08715, doi:10.1029/2008GL033611.
- Keeling, C. D., and T. P. Whorf (1997), Possible forcing of global temperature by the oceanic tides, *Proc. Natl. Acad. Sci. U. S. A.*, 94, 8321–8328.
- Kolker, A. S., and S. Hameed (2007), Meteorologically driven trends in sea level rise, *Geophys. Res. Lett.*, 34, L23616, doi:10.1029/2007GL031814.
- Pugh, D. T. (1982), A comparison of recent and historical tides and mean sea-levels of Ireland, *Geophys. J. R. Astron. Soc.*, 71, 809–815.
- Pugh, D. T. (2004), *Changing Sea Levels Effects of Tides, Weather and Climate*, Cambridge Univ. Press, Cambridge, U. K.
- Ray, R. D. (2006), Secular changes of the  $M_2$  tide in the Gulf of Maine, *Cont. Shelf Res.*, 26, 422–427.
- Ray, R. D. (2007), Decadal climate variability: Is there a tidal connection?, *J. Clim.*, 20, 3542–3560, doi:10.1175/JCLI4193.1.
- Woodworth, P. L., S. M. Shaw, and D. L. Blackman (1991), Secular trends in mean tidal range around the British Isles and along the adjacent European coastline, *Geophys. J. Int.*, 104, 593–609.
- Yasuda, I., S. Osafune, and H. Tatebe (2006), Possible explanation linking 18.6-year period nodal tidal cycle with bi-decadal variations of ocean and climate in the North Pacific, *Geophys. Res. Lett.*, 33, L08606, doi:10.1029/2005GL025237.

D. A. Jay, Department of Civil and Environmental Engineering, Portland State University, Portland, OR 97207, USA. (djay@cecs.pdx.edu)